REPRODUCTION
RESEARCH

Membrane trafficking directed by VAMP2 and syntaxin 3 in uterine epithelial cells

Sadaf N Kalam[1], Louise Cole[2], Laura Lindsay[1] and Christopher R Murphy[1]

[1]*Anatomy and Histology, School of Medical Sciences and the Bosch Institute, The University of Sydney, Sydney, New South Wales, Australia and* [2]*The ithree Institute, Institute of Infection, Immunity and Innovation, University of Technology Sydney, Sydney, New South Wales, Australia*

Correspondence should be addressed to S N Kalam; Email: sadaf.kalam@sydney.edu.au

Abstract

Luminal uterine epithelial cells (UEC) have a surge in vesicular activity during early uterine receptivity. It has been predicted these vesicles exit the UEC via exocytosis resulting in secretion and membrane trafficking. The present study investigated the changes in SNARE proteins VAMP2 (v-SNARE) and syntaxin 3 (t-SNARE) localisation and abundance in UECs during early pregnancy in the rat. We found VAMP2 and syntaxin 3 are significantly higher on day 5.5 compared to day 1 of pregnancy. On day 5.5, VAMP2 is perinuclear and syntaxin 3 is concentrated in the apical cytoplasm compared to a cytoplasmic localisation on day 1. This change in localisation and abundance show VAMP2 and syntaxin 3 are involved in vesicular movement and membrane trafficking in UECs during early pregnancy. This study also investigated the influence of cytoskeletal disruption of microtubules and actin filaments on VAMP2 and syntaxin 3 in UECs grown in vitro, since microtubules and actin influence vesicle trafficking. As expected, this study found disruption to microtubules with colchicine and actin with cytochalasin D impacted VAMP2 and syntaxin 3 localisation. These results suggest VAMP2 and syntaxin 3 are involved in the timely trafficking of vesicular membranes to the apical surface in UECs during early pregnancy, as are of microtubules and actin.

Reproduction (2020) **160** 533–546

Introduction

Uterine receptivity involves many changes to the surface of the uterine epithelial cells (UEC) (Ljungkvist 1972, Nilsson & Lundkvist 1979, Dey *et al.* 2004). These morphological and molecular changes are referred to collectively as 'the plasma membrane transformation' and include loss of microvilli, loss of apical terminal web and an increase in apical lipid rafts and adhesion proteins (Murphy & Shaw 1994, Murphy 2004). These changes are likely to be mediated by membrane trafficking via vesicle transport. Indeed, previous studies have shown an increase in the number of apical vesicles in UECs at the time of receptivity, the same time these apical membrane changes are occurring (Parr 1982).

Uterine receptivity is required for blastocyst implantation. Implantation in rats and humans involves apposition of the blastocyst to UECs, adhesion and then penetration through the epithelium and basal lamina, resulting in invasion into the stromal vasculature (Schlafke & Enders 1975, Schlafke *et al.* 1985). During apposition, it is well known that there is a surge in the number of apical vesicles that eventually incorporate into the apical plasma membrane (Parr 1982, Murphy 1993). However, it has yet to be investigated how polarised membrane trafficking re-organises the apical surface to facilitate blastocyst implantation.

Membrane trafficking involves budding vesicles from donor membranes and then vesicle fusion with their respective target membranes with the assistance of Soluble NsF (N-ethylmaleimide sensitive factor) attachment proteins (SNAPs) and SNAP receptors (SNARE) proteins (Almers & Tse 1990, Lindau & Almers 1995, Band & Kuismanen 2005). SNARE proteins are a group of proteins that are involved in intracellular membrane trafficking. The SNARE machinery involves pairing a vesicle SNARE (v-SNARE) with a target SNARE (t-SNARE) which pulls the opposing membranes together resulting in membrane fusion (Fig. 1) (Söllner *et al.* 1993, Sutton *et al.* 1998).

Vesicle associated membrane protein 2 (VAMP2) is a v-SNARE protein involved in vesicle docking and fusion (Tajika *et al.* 2007). VAMP2 was first discovered in the rat brain, where it plays a key role in the fusion of synaptic vesicles (Baumert *et al.* 1989). VAMP2 was also found in non-neural tissue where it participates in regulated exocytosis of vesicles in adipocytes and renal epithelial cells (Rossetto *et al.* 1996, Takata *et al.* 2004, Watson *et al.* 2004).

ISSN 1470–1626 (paper) 1741–7899 (online)
https://doi.org/10.1530/REP-20-0233
Online version via https://rep.bioscientifica.com

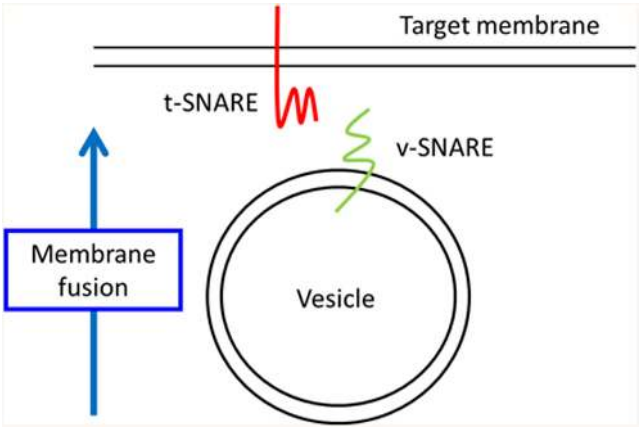

Figure 1 Schematic diagram showing the pairing of v-SNARE and t-SNARE involvement in membrane fusion.

Syntaxin 3, a t-SNARE, was found in polarised epithelial cells and is involved in delivery of proteins from the *trans*-Golgi apparatus to the apical surface and to apical membrane recycling (Low *et al.* 1998, ter Beest *et al.* 2005). Syntaxin 3 has been located in the apical and basolateral plasma membrane in epithelial cells (Low *et al.* 1996, Sharma *et al.* 2006, Soo Hoo *et al.* 2016). Syntaxin 3 has also been shown to be compartmentalised to the apical domain in polarised cells, such as human intestinal cells and MDCK cells, suggesting a function in polarised membrane trafficking (Delgrossi *et al.* 1997). Syntaxin 3 localisation is thought to be dependent on microtubule and actin filaments, as disruption of these cytoskeletal elements have led to mislocalisation of syntaxins in MDCK cell lines and NRK cell lines (Kreitzer *et al.* 2003, Low *et al.* 2006, Sharma *et al.* 2006).

It is well known that vesicles bud off from the Golgi apparatus and move along the microtubules until they reach the target membrane, where they fuse spontaneously or are directed into fusion by a t-SNARE (Weber *et al.* 1998, Duman & Forte 2003, Ungermann & Langosch 2005, Jahn & Scheller 2006, Jena 2011). Regulated polarised membrane trafficking is dependent on timely fusion and is almost always controlled by t-SNAREs (Soo Hoo *et al.* 2016).

The present study investigated the changes in VAMP2 (v-SNARE) and syntaxin 3 (t-SNARE) localisation and abundance in UECs during early pregnancy in the rat. Since there is a rise in vesicular activity in UECs during the time of receptivity, we hypothesise that there should be a change in the abundance of these SNARE proteins. The influence of cytoskeleton disruption of microtubules and actin filaments on VAMP2 and syntaxin 3 in HEC1A (non-receptive) and RL95-2 (receptive) UECs in vitro was also investigated since microtubules and actin play a key role in vesicle trafficking. HEC1A cell lines are classified as non-receptive since, in the presence of trophoblast cells, they display poor adhesive properties similar to non-receptive UECs found globally in the rat uterus, thus making them a good model for non-receptive UECs. In the presence of blastocyst, RL95-2 cells show high adhesive properties similar to receptive UECs throughout the rat uterus, hence a suitable model for receptive UECs (Martín *et al.* 2000, Hannan *et al.* 2010). It is further hypothesised that VAMP2 and syntaxin 3 will change their localisation and abundance during uterine receptivity in vivo and the disruption of the cytoskeleton will also affect the localisation and abundance of VAMP2 and syntaxin 3 in vitro.

Materials and methods

Animals and mating

This study used female virgin Wistar rats aged 10–12 weeks, and all procedures were approved by The University of Sydney Animal Ethics Committee. Rats were housed in plastic cages at 21°C under a 12 h light:12 h darkness cycle and were provided with free access to food and water. Pro-oestrus female rats were mated overnight with males of proven fertility. The presence of sperm in a vaginal smear the morning after indicated successful mating and this was designated day 1 of pregnancy. Uterine tissues were collected from five rats each from days 1, 3.5, 5.5, 6 and 7 of pregnancy.

Tissue collection

Rats were administered 20 mg/kg of sodium pentobarbitone (Vibac Animal Health, NSW, Australia) intraperitoneally and the uterine horns were collected under deep anaesthesia, before killing. The uterine horns were then randomly allocated for immunofluorescence and Western blotting.

Indirect immunofluorescence microscopy of the rat uterus

Uterine horns (5 mm long pieces) were coated with the cryo-protectant Tissue Tek OCT (Sakura Fineteck, USA), before being snap-frozen in super-cooled isopentane, and stored in liquid nitrogen until required. Frozen sections (7 µm) were cut using a Leica CM 3050 cryostat (Leica) and air-dried on gelatine-chrome alum-coated slides.

Sections of inter-implantation sites were then fixed in 4% paraformaldehyde in 0.1 M PBS (pH 7.4) for 10 min at room temperature (RT), washed with PBS and blocked with 1% BSA (Sigma Aldrich) in PBS for 30 min at RT. Sections were incubated overnight at 4°C with mouse monoclonal (6F9) VAMP2 (20 µg/mL; Abcam, ab181754) and rabbit monoclonal syntaxin 3 (0.46 µg/mL; Abcam: ab133750), diluted in 1% PBS/BSA. Concurrently, control sections were also incubated with non-immune IgG (Sigma Aldrich) at the same concentration as primary antibodies. Sections were washed in PBS and incubated with anti-rabbit IgG (whole molecule, F (ab′)$_2$ fragment Cy3 (0.33 µg/mL; Sigma Aldrich) and FITC-conjugated goat anti-mouse IgG (3 µg/mL; Jackson ImmunoResearch) for 30 min at RT. Sections were washed in

PBS and mounted with Vectashield containing DAPI (Vector Laboratories, CA, USA) and cover slipped prior to microscopy.

A Zeiss AxioImager Microscope (Carl Zeiss) was used to image the sections and Z-stack images were acquired with the use of Zeiss AxioCam HR digital monochrome CCD camera (Carl Zeiss) and ZEN 2013 (Blue edition) software (Carl Zeiss). DAPI, FITC and Cy3 filters were used together with 20× and 60× oil objectives. The Z-stacks were then deconvolved using the Nearest Neighbour deconvolution algorithm in the ZEN software.

Cell culture

HEC1A cells, a non-receptive human endometrial adenocarcinoma cell line (ATCC HTB-112™), were grown at 37°C in 5% CO_2 in McCoy's 5A Medium (1×)/L-glutamine (GIBCO) supplemented with 10% fetal bovine serum (Bovogen Biologicals Pty, Essendon, VIC, Australia) and 1% streptomycin and penicillin (Invitrogen) until confluent.

RL95-2 cells, a receptive human endometrial adenocarcinoma cell line (ATCC CRL-1671™), were grown at 37°C in 5% CO_2 in DMEM/F-12 (Dulbecco's Modified Eagle Medium/Nutrient Mixture F-12) containing HEPES and L-glutamine (GIBCO) supplemented with 10% fetal bovine serum (Bovogen Biologicals Pty), 0.005 mg/mL insulin (I0516-5ML, Sigma Aldrich) and 1% streptomycin and penicillin (Invitrogen) until confluent.

Confluent cells were treated with either colchicine (3 µg/mL; Sigma Aldrich) or cytochalasin D (3 µg/mL; Sigma Aldrich) for 18 h and washed with PBS to deactivate the treatment.

Immunofluorescence labelling and confocal microscopy of UECs grown in vitro

Confluent monolayer cells grown on No. 1 thickness coverslips were fixed with 2% paraformaldehyde for 20 min at RT. Cells were washed in PBS and incubated with 100 mM glycine for 30 min at RT, permeabilised with 0.1% Triton for 5 min and incubated with a 2%BSA/PBS/0.1% Triton blocking solution for 1 h at RT. Cells were incubated with mouse monoclonal (6F9) VAMP2 (20 µg/mL; Abcam, ab181754) or rabbit monoclonal syntaxin 3 (0.46 µg/mL; Abcam, ab133750), diluted in blocking solution and incubated, at 4°C overnight. Control cells were incubated with non-immune IgG (Sigma Aldrich) at the same concentration as primary antibodies. Cells were washed with PBS and incubated with secondary antibody FITC-conjugated goat anti-mouse IgG (3 µg/mL; Jackson ImmunoResearch Laboratories) or FITC-conjugated AffiniPure goat anti-rabbit IgG secondary antibody (2.5 µg/mL; Jackson ImmunoResearch Laboratories), as appropriate, for 30 min at RT. All cells on coverslips were subsequently washed in PBS and mounted with Vectashield containing DAPI (Vector Laboratories) onto glass slides. Z-series optical sections of the cells were taken with a 100× objective (Plan-Apochromat 100×/NA 1.40 Oil DIC M27/WD 0.17 mm) on Zeiss LSM 510 Meta Confocal microscope (Carl Zeiss) and images were acquired using the Zeiss LSM software (Carl Zeiss). Confocal microscopy allowed the spatial localisation of both VAMP2 and syntaxin 3, in UECs grown in vitro, to be probed further.

Isolation of rat uterine luminal epithelial cells

UECs were isolated in the entire uterine horn consisting of implantation and inter-implantation sites as previously described (Kaneko *et al.* 2008) and immediately placed into lysis buffer (50 mM Tris–HCl, pH 7.5, 1 mM EDTA, 150 mM NaCl, 0.1% SDS, 0.5% Deoxycholic acid, 1% Igepal and 1% protease inhibitor cocktail; Sigma Mammalian Cell lysis kit, Sigma Adrich) with 10% PhosSTOP phosphatase inhibitor (Roche). The isolated cells were homogenised using a 23-gauge needle and a 1-mL syringe (Livingstone International, Rosebery, NSW, Australia) and centrifuged at 8000 ***g*** at 4°C for 3 min. The supernatant was collected and frozen immediately in liquid nitrogen and stored at −80°C until use.

Cell culture lysate for western blot analysis

Confluent cells were processed with lysis buffer (50 mmol/L Tris-HCl, pH 7.5, 1 mmol/L EDTA, 150 mmol/L NaCl, 0.1% SDS, 0.5% deoxycholic acid, 1% igepal, and 1% protease inhibitor cocktail; Mammalian Cell lysis kit; Sigma Aldrich) with 10% PhosSTOP phosphatase inhibitor (Roche), homogenised using a 23-gauge needle and a 1-mL syringe (Livingstone International), and briefly centrifuged at 8000 ***g*** at 4°C for 3 min. The supernatant was collected and frozen immediately in liquid nitrogen and stored at −80°C until use.

Western blot analysis

Protein concentrations were determined using the BCA protein assay (Micro BCA™ protein assay kit; Thermo Fisher Scientific) and CLARIOstar microplate reader (BMG labtech Durham, NC, USA) according to the manufacturer's instructions. Protein samples (20 µg) and sample buffer (8% glycerol, 50 mM Tris–HCl, pH 6.8, 1.6% SDS, 0.024% bromophenol blue, 4% β-2-mercaptoethanol) were heated at 95°C for 5 min prior to loading onto a 4–20% pre-cast SDS-polyacrylamide gel (Mini PROTEAN TGx Stain-Free™ gels; Bio-Rad Laboratories; cat# 456-8095). The proteins were separated through electrophoresis at 200 V for 40 min and transferred to a polyvinylidene dilfluoride (PVDF) membrane (Immunobilon™ transfer membrane; Millipore) at 100 V for 1 h 30 min. Membranes were blocked with 2% skim milk in TBS-t (10 mM Tris–HCl, pH 7.4, 150 mM NaCl and 0.05% Tween 20) for 1 h RT with constant agitation and incubated with primary antibodies (1 µg/mL mouse monoclonal (6F9) VAMP2 (Abcam, ab181754) or 0.0115 µg/mL rabbit monoclonal syntaxin 3, Abcam, ab133750), diluted in 1% skim milk in TBS-t overnight at 4°C on a rocking platform. The membranes were washed in TBS-t and subsequently incubated for 2 h with goat anti-rabbit IgG horseradish peroxidase (HRP)-conjugated secondary antibody (0.5 µg/mL; Dako) or sheep anti-mouse polyclonal HRP-linked IgG secondary antibody (1 µg/mL; GE Healthcare) at RT with constant agitation. Protein bands were detected with the use of Immobilon Western HRP Substrate (Merck Millipore) and captured using a CCD camera and Bio-Rad ChemiDoc MP System (Bio-Rad). Membranes were then incubated in stripping buffer (62.5 mM Tris–HCl (pH 6.7), 2% SDS and 100 mM β-mercaptoethanol) at 60°C for 45 min and

re-probed with mouse monoclonal anti-β-actin antibody (0.4 µg/mL; Sigma Aldrich) overnight at 4°C followed by HRP-conjugated goat anti-mouse IgG (0.2 µg/mL; GE Healthcare) for 2 h at RT, to ensure equal loading.

Densitometry analysis

Protein band intensities were quantified using the Volume Analysis Tool with local background subtraction using the Bio-Rad Image Lab 4.0 software (Bio-Rad) and normalised to β-actin band intensities from the same lane. Statistical analysis was performed on normalised intensities with GraphPad Prism Software (Version 6.04, GraphPad Software, Inc.). Changes in quantity from day 1, 3.5, 5.5, 6 and 7 of pregnancy were analysed using ordinary one-way ANOVA. For multiple comparisons Tukey's post hoc test was applied (reporting multiplicity-adjusted *P*-values) to determine which pairs of means were significantly different. Changes in abundance between HEC1A and RL95-2 were analysed using a Student's *t*-test. In cytochalasin D and colchicine treated samples, quantity comparisons were made between untreated and treated samples and also analysed using Student's *t*-test. $P < 0.05$ was determined to be significant. All graphs were generated using GraphPad Prism Software and error bars representing mean ± S.E.M.

Results

SNARE proteins in early pregnancy in vivo (rat uterus)

Indirect immunofluorescence and Western blot analysis revealed that VAMP2 and syntaxin 3 are present in UECs on days 1, 3.5, 5.5, 6 and 7 of pregnancy (Figs 2 and 3). On day 1 of pregnancy, VAMP2 and syntaxin 3 were diffusely located throughout the cytoplasm of UECs (Fig. 2A, B and C). On day 3.5, VAMP2 was localised in clusters in the perinuclear cytoplasmic areas and syntaxin 3 could be seen in the apical region above VAMP2 (Fig. 2D, E and F). On days 5.5 and 6, VAMP2 was further localised to the perinuclear region of the cytoplasm, whereas syntaxin 3 was strongly present in the apical region compartmentalised above VAMP2 (Fig. 2G, H, I, J, K and L). On day 7, VAMP2 returned to its cytoplasmic localisation throughout the cell (as seen in day 1) but syntaxin 3 remained in the apical region (Fig. 2M, N and O). Low magnification images of day 5.5 showing VAMP2 and syntaxin 3 staining (Fig. 2P, Q and R). Western blot analysis found VAMP2 (19 kDa) and syntaxin 3 (33 kDa) present on all days of early pregnancy at their expected band sizes and both are significantly greater on day 5.5 compared to days 1 and 3.5 (Fig. 3).

SNARE proteins present in vitro (human endometrial epithelial cell lines)

Immunofluorescence confocal microscopy allowed the precise localisation of VAMP2 and syntaxin 3 to be probed further; this technique also confirmed that VAMP2 and syntaxin 3 was present in both HEC1A and RL95-2 cell lines (Figs 4 and 5). VAMP2 was localised (shown by a low level of diffuse punctate staining) to the cytoplasm in both HEC1A and RL95-2 cell lines. In HEC1A (Fig. 4A, B, C, D and E), there appeared to be more punctate staining of VAMP2 throughout the cells compared to that seen in RL95-2 cells. It is also noteworthy that the diameter of the individual punctate aggregates is larger than those in RL95-2 cells (Fig. 4F, G, H, I and J). In comparison to VAMP2, syntaxin 3 was present in HEC1A cells and appeared to be localised to the plasma membrane primarily and the cytoplasm (Fig. 5A, B, C, D and E). However, in RL95-2 cells, syntaxin 3 was shown by punctate staining in both the cytoplasm and the plasma membrane; labelling was also localised primarily to the plasma membrane (Fig. 5F, G, H, I and J).

Western blot analysis found VAMP2 (19 kDa) and syntaxin 3 (33 kDa) were present in UECs in vitro (Fig. 6A and B). VAMP2 was significantly greater in abundance in HEC1A cells compared to RL95-2 (Fig. 6C), whereas syntaxin 3 was significantly greater in RL95-2 cells (Fig. 6D).

The effect of the anti-microtubule drug colchicine on SNARE proteins

When treated with colchicine, a microtubule polymerisation inhibitor (Scott 1960), the localisation of both VAMP2 and syntaxin 3 was altered in both HEC1A and RL95-2 cell lines (Figs 7 and 8). In colchicine treated HEC1A cells, VAMP2 appeared in punctate cytoplasmic clusters and is sparse in colchicine treated RL95-2 cells (Fig. 7A, B, C, D, E, F, G, H, I and J). Syntaxin 3 in colchicine treated HEC1A cells was found in all areas of the plasma membrane and cytoplasm (Fig. 8A, B, C, D and E). In colchicine treated RL95-2 cells, syntaxin 3 is also found in the plasma membrane and the cytoplasm (Fig. 8F, G, H, I and J).

Localisation of SNARE proteins is dependent on actin

Similar to the effect of colchicine, cytochalasin D treatment which inhibits actin polymerisation (Goddette & Frieden 1986) also affected the localisation of both VAMP2 and syntaxin 3 in both HEC1A and RL95-2 cells (Figs 9 and 10). VAMP2 was localised in small punctate cytoplasmic clusters in both HEC1A and RL95-2 cells (but to a lesser extent) when treated with cytochalasin D (Fig. 9A, B, C, D, E, F, G, H, I and J). Syntaxin 3, in HEC1A cells, was located primarily at the plasma membrane and to some extent seen in the cytoplasm in a punctate-like fashion (Fig. 10A, B, C, D and E). Interestingly in RL95-2 cells, syntaxin 3 could no longer be detected at the plasma membrane, instead labelling appeared to be confirmed to perinuclear patches in the cytoplasmic in some areas (Fig. 10F, G, H, I and J).

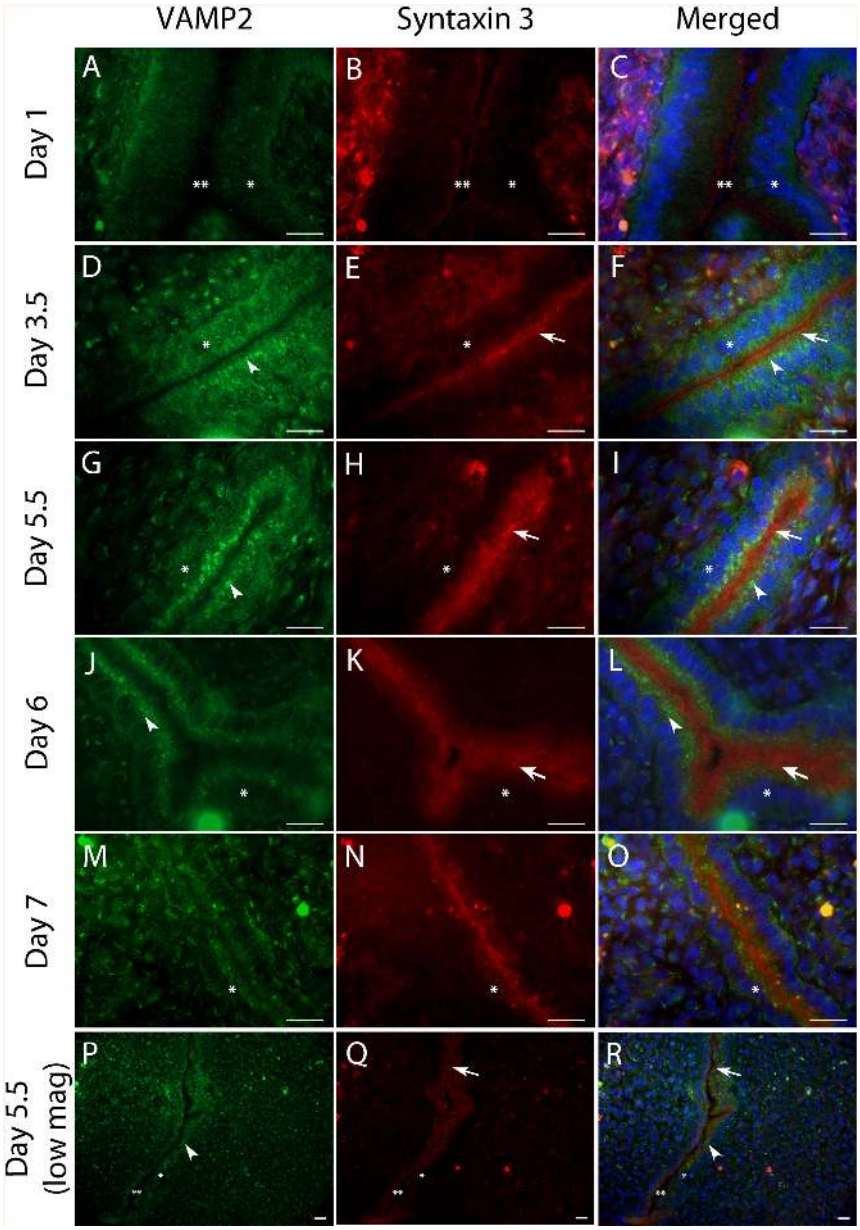

Figure 2 VAMP2 and syntaxin 3 localisation in rat uterine epithelial cells (UEC) in early pregnancy. (A, B and C) On day 1 of pregnancy, VAMP2 (green) and syntaxin 3 (red) labelling was localised to the cytoplasm throughout the UECs with very little staining. (D, E and F) On day 3.5, VAMP2 was localised in the cytoplasm shown by clear perinuclear staining; syntaxin 3 appeared to localise apically. On days 5.5 (G, H and I) and 6 (J, K and L), VAMP2 was intensely stained in the perinuclear region (arrowheads) of the cytoplasm and syntaxin 3 was strongly localised in the apical region (arrows), distinct from VAMP2 in UECs. (M, N and O) On day 7, VAMP2 returned to its cytoplasmic localisation throughout the UECs and syntaxin 3 remained in the apical region. Low magnification images of VAMP2 and syntaxin 3 on day 5.5 (P, Q and R). DAPI labelled nuclei (blue) can be seen in the overlay images: C, F, I, L, and O. All scale bars are 20 µm. *Epithelium, **Lumen.

Western blot analysis of treated UECs in vitro

Western blot analysis found a significant increase in VAMP2 (19 kDa) in colchicine treated HEC1A cells compared to non-treated cells and an increased trend in VAMP2 in HEC1A cells when treated with cytochalasin D (Fig. 11).

Western blot analysis of syntaxin 3 (33 kDa) found a higher trend in both HEC1A and RL95-2 colchicine treated cells compared to untreated cells (Fig. 12A, B, C and D). There is also an increased trend of syntaxin 3 in HEC1A and RL95-2 cells when actin was disrupted compared to untreated cells (Fig. 12A, B, E and F). However, syntaxin 3 is only significantly greater in colchicine treated RL95-2 cells compared to untreated RL95-2 cells (Fig. 12D and E).

Treatment validation and controls

Cytochalasin D treated cells were validated with Phalloidin (Fig. 13A and B) and colchicine treated cells were validated with β-tubulin staining to confirm that these cytoskeletal inhibitory drugs disrupted both actin and microtubules (Fig. 13C and D). Non-immune and negative controls were performed alongside all experimental runs and showed no staining (Fig. 13E and F). Representative images are shown in Fig. 13.

Discussion

This study has demonstrated for the first time that the v-SNARE, VAMP2 and t-SNARE, syntaxin 3 are both present in UECs during early pregnancy in the rat and

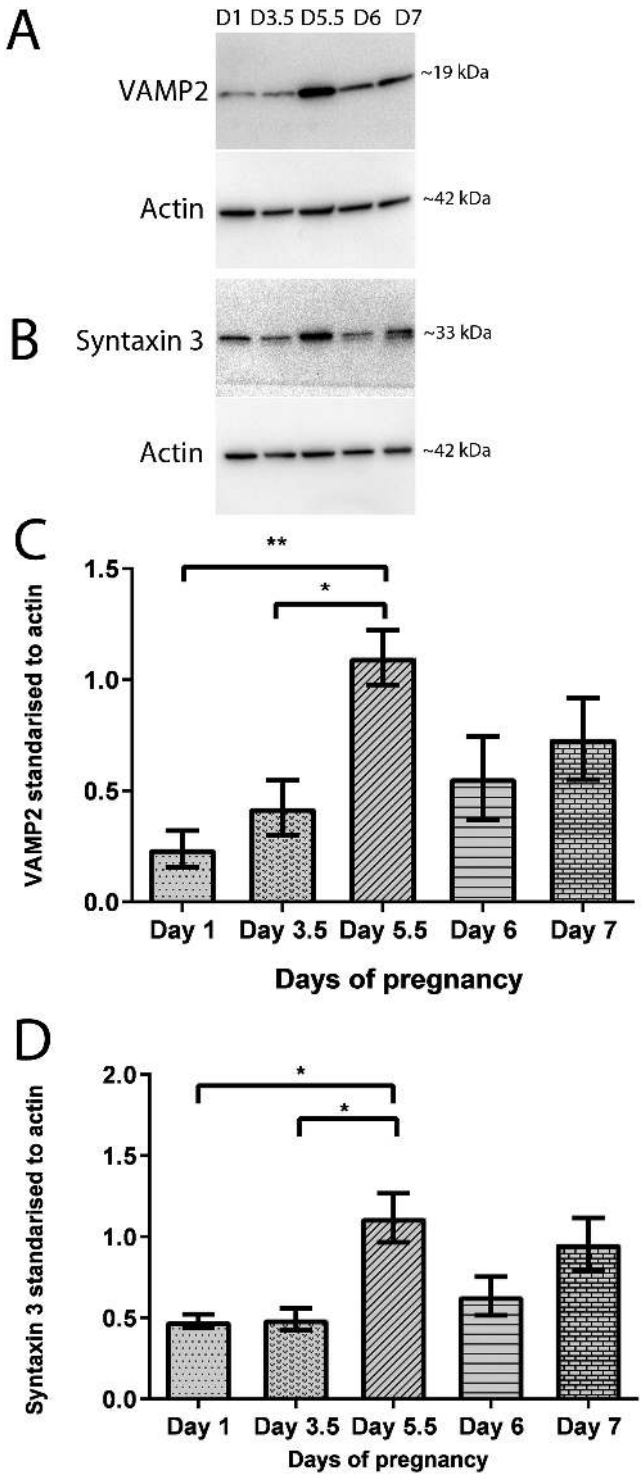

Figure 3 Western blot analysis of VAMP2 and syntaxin 3 in isolated UECs. (A) VAMP2 was present as a 19-kDa band and syntaxin 3 as a 33-kDa band (B) in isolated UECs on days 1, 3.5, 5.5, 6 and 7 of pregnancy. Actin (42-kDa band) was used as a loading control. Densitometric and statistical analysis (one-way ANOVA) found a significant increase in (C) VAMP2 and (D) syntaxin 3 on day 5.5 compared to day 1 and day 3.5; $^{*}P < 0.05$; $^{**}P < 0.01$. Error bar is the mean ± S.E.M., $n = 5$.

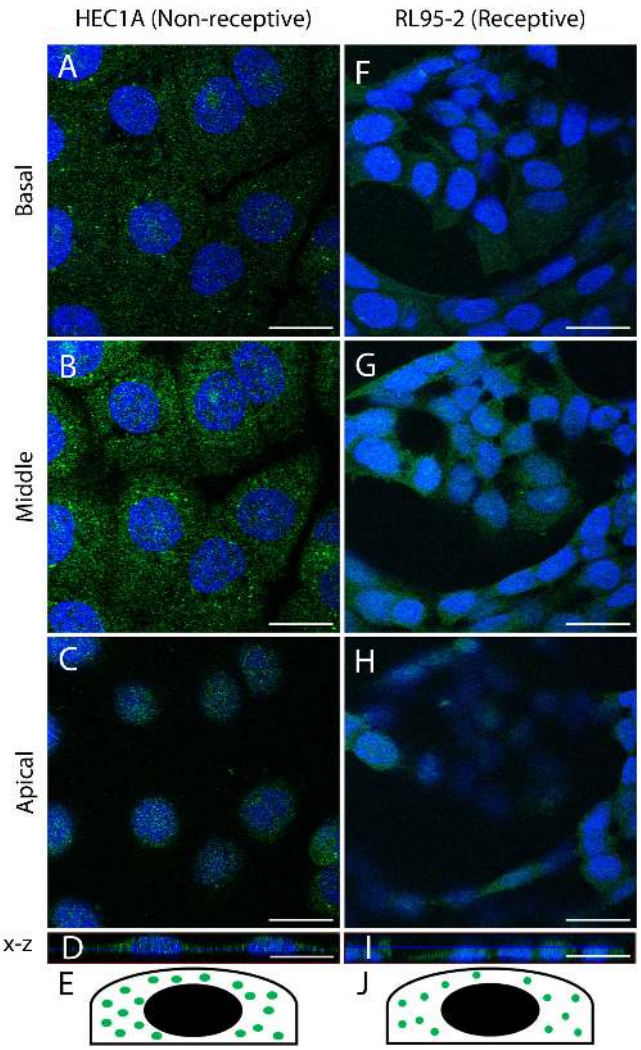

Figure 4 Immunofluorescence confocal microscopy showing VAMP2 localisation in HEC1A and RL95-2 cells. (A–D) HEC1A cells showed VAMP2 was cytoplasmic with prominent punctate staining. (F–I) VAMP2 was cytoplasmic in RL95-2. (D and I) XZ orthogonal plane of Z-stack. (E and J) Schematic diagrams representing VAMP2 localisation in these cells taken from the Z-plane. Scale bars: 20 µm.

in cultured UECs in vitro and moreover with differing localisation and abundance during the early stage of pregnancy. Western blotting data clearly showed that both VAMP2 and syntaxin 3 abundance is significantly increased during the apposition stage of implantation (day 5.5) compared to all other days of early pregnancy. The localisation of these SNARE proteins in the apical cytoplasm suggests polarised membrane trafficking via exocytosis is taking place in preparation for uterine receptivity.

This study also found increased perinuclear localisation of VAMP2 and a significant increase in VAMP2 abundance on day 5.5 (apposition stage). This is consistent with studies in other cells where VAMP2 was also found in this peri-nuclear region in

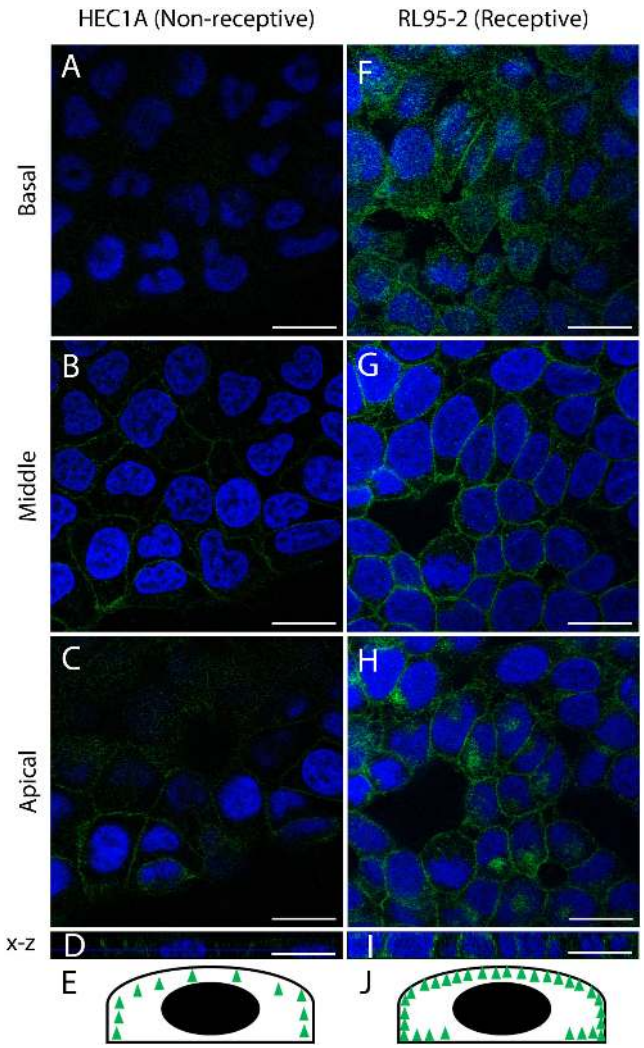

Figure 5 Immunofluorescence confocal microscopy showing syntaxin 3 localisation in HEC1A and RL95-2 cells. (A–D) Syntaxin 3 in HEC1A cells was localised primarily to the plasma membrane with some staining in the cytoplasm. (F–I) In RL95-2 cells, syntaxin 3 was localised in a punctate fashion in both the plasma membrane and cytoplasm. (D and I) XZ orthogonal plane of Z-stack. (E and J) Schematic diagrams representing syntaxin 3 localisation in the cells taken from the Z-plane. Scale bars: 20 µm.

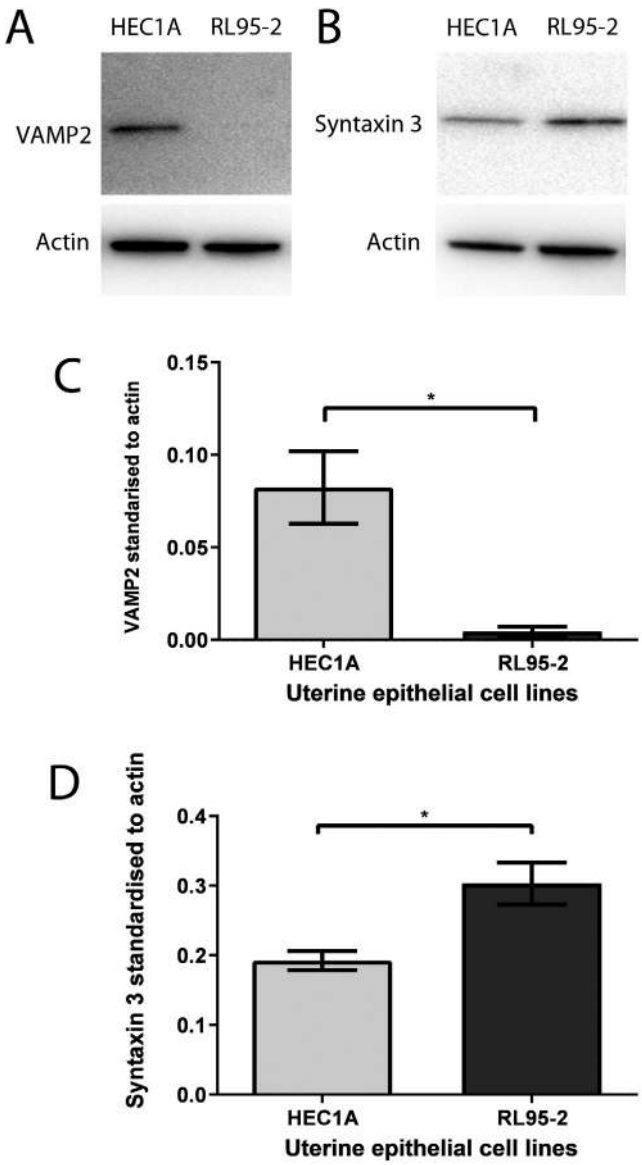

Figure 6 Western blot analysis of VAMP2 and syntaxin 3 in human endometrial cell lines. (A) VAMP2 was present at 19 kDa and (B) syntaxin 3 at 33 kDa in human endometrial cell lines. Actin (42 kDa) was used as a loading control. Densitometry analysis and statistical analysis (Student's *t*-test) revealed the total quantity of (C) VAMP2 was significantly high in HEC1A cells compared to RL95-2 and (D) syntaxin 3 was significantly higher in RL95-2 cells compared to HEC1A; $^*P < 0.05$. Error bar is the mean ± S.E.M., $n = 5$.

myoblast and juxtaglomerular cells (Randhawa *et al.* 2000, Mendez *et al.* 2011). Vesicles are generated with VAMP2 embedded in their membranes at the *trans*-Golgi apparatus near the nucleus, thereby resulting in peri-nuclear staining (Randhawa *et al.* 2000, Dugani *et al.* 2008). This suggests membranes of exocytotic vesicles produced at the time of apposition are coming from the *trans*-Golgi apparatus due to the presence of this v-SNARE (Martinez-Arca *et al.* 2000, Dugani *et al.* 2008). The involvement of VAMP2 in exocytosis is not necessary for membrane fusion; however, its presence means that membrane fusion will take place at a faster rate. VAMP2 knockout studies looking at synaptic areas found fast calcium triggered fusion decreased by more than 100 fold (Schoch *et al.* 2001). Thus, this significant increase of VAMP2 found in UECs at apposition implies fast membrane fusion is taking place. On day 6 (adhesion stage), there is a rapid change in the morphological and molecular composition of the apical membrane that is most likely assisted by this rapid membrane fusion directed by VAMP2 (Schoch *et al.* 2001). The swift turnover of the apical surface that occurs during uterine receptivity is vital to implantation which only takes place during a short window of receptivity and which we now

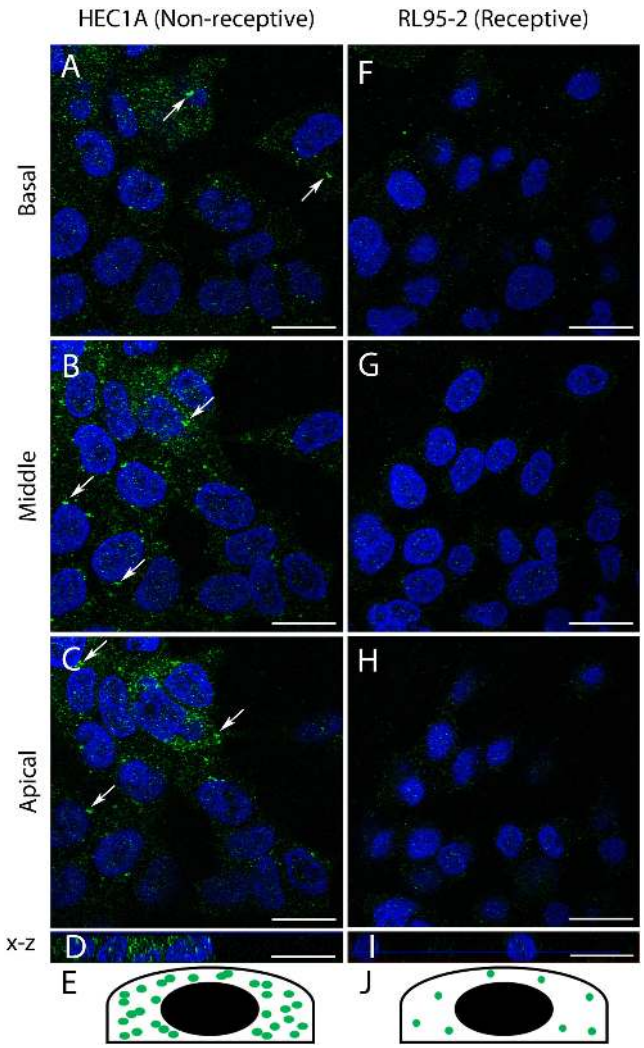

Figure 7 Immunofluorescence confocal microscopy showing VAMP2 localisation in HEC1A and RL95-2 cells treated with colchicine. (A–D) In HEC1A cells, VAMP2 was found in punctate cytoplasmic clusters (arrows). (F–I) In RL95-2 cells, VAMP2 was sparsely found in the cytoplasm. (D and I) XZ orthogonal plane of Z-stack. (E and J) Schematic diagrams representing VAMP2 localisation in the cells taken from the Z-plane. Scale bars: 20 µm.

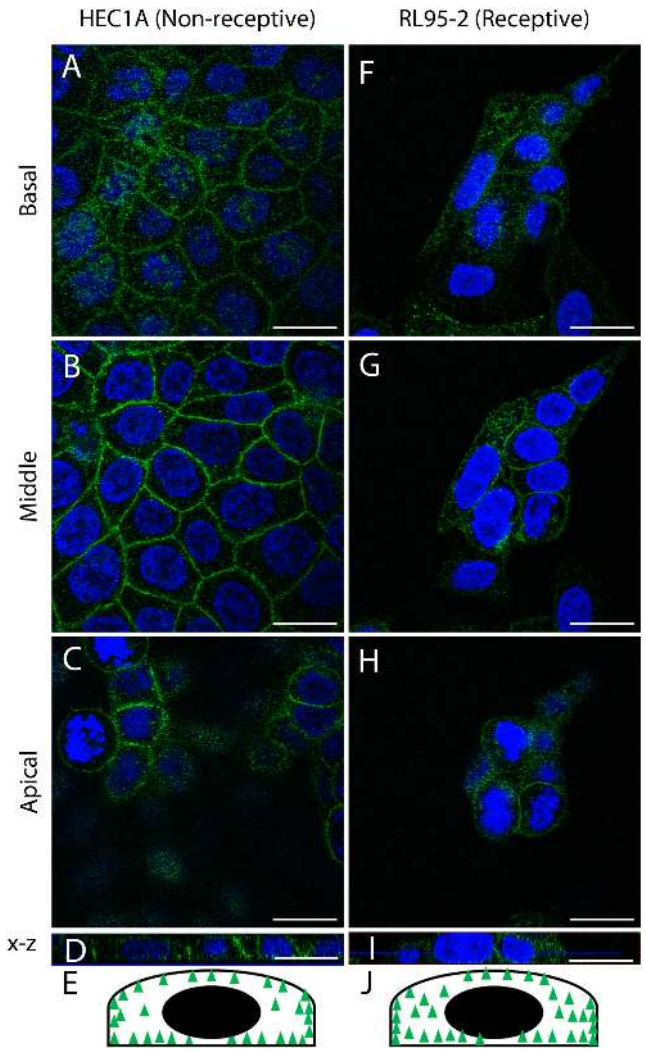

Figure 8 Immunofluorescence confocal microscopy showing syntaxin 3 localisation in HEC1A and RL95-2 cells treated with colchicine. (A–D) Syntaxin 3 in colchicine treated HEC1A cells was found in all areas of the plasma membrane and cytoplasm. (F–I) In colchicine treated RL95-2 cells, syntaxin 3 was also found in the plasma membrane and the cytoplasm. (D and I) XZ orthogonal plane of Z-stack. (E and J) Schematic diagrams representing VAMP2 localisation in the cells taken from the Z-plane. Scale bars: 20 µm.

show is likely mediated by this VAMP2 associated rapid membrane fusion.

Vesicular membranes with VAMP2 are known to also carry aquaporin 2 in kidney collecting duct epithelium and GLUT4 in muscle, adipocytes and myoblast cells (Nielsen *et al.* 1995, Martinez-Arca *et al.* 2000, Ramm *et al.* 2000, Randhawa *et al.* 2000, Watson & Pessin 2001, Dugani *et al.* 2008). Previous studies have found aquaporin 2 is present on the surface of human UECs during the mid- and late secretory phase, implying a role in fluid movement during implantation (Hildenbrand *et al.* 2006). GLUT4 is another protein that associates with VAMP2. During the period between blastocyst formation and implantation, GLUT4 is thought to play a pivotal role in meeting the energy requirements of the embryo (Korgun *et al.* 2001). Embryonic fuel metabolism switches its preferred substrate from the more oxidized pyruvate to glucose during early blastocyst formation and this is signalled by GLUT4 (Pantaleon & Kaye 1998). Thus, having VAMP2 in exocytotic vesicles could promote fusion of these important membrane proteins to the apical surface of UECs via interaction with a t-SNARE, such as syntaxin 3.

T-SNARE syntaxin 3 interacts with v-SNARE VAMP2 in the SNARE complex that drives membrane fusion (Peng *et al.* 1997, Karvar *et al.* 2005). Membrane enclosed vesicles with v-SNAREs that bud off from

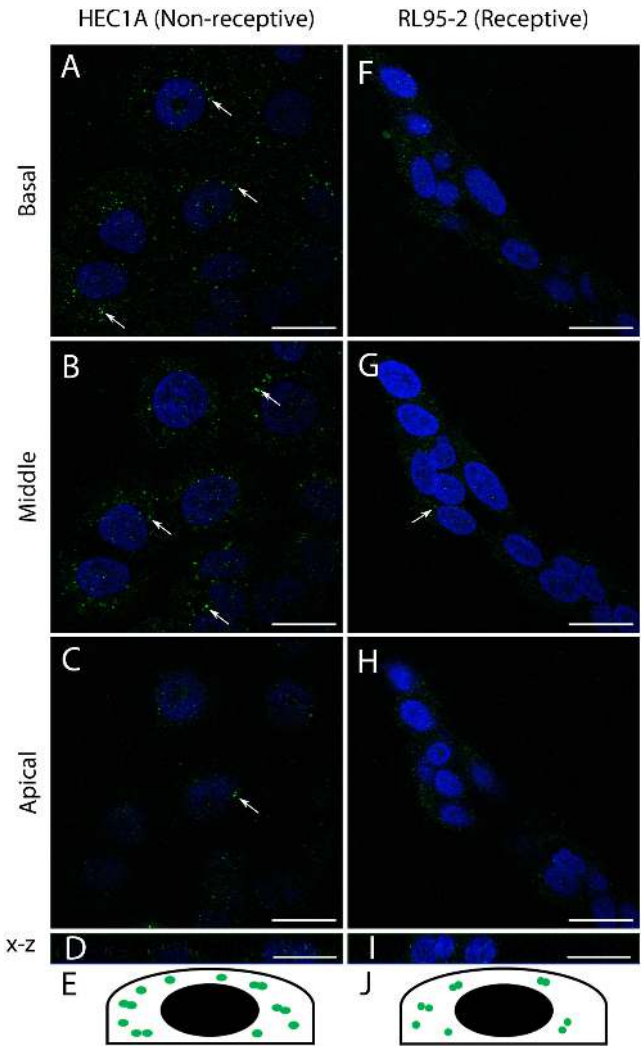

Figure 9 Immunofluorescence confocal microscopy showing VAMP2 localisation in HEC1A and RL95-2 cells treated with cytochalasin D. (A–I) VAMP2 immunofluorescence was localised in small punctate clusters (arrows) cytoplasmically in both HEC1A and RL95-2 cells when treated with cytochalasin D. (D and I) XZ orthogonal plane of Z-stack. (E and J) Schematic diagrams representing VAMP2 localisation in the cells taken from the Z-plane. Scale bars: 20 µm.

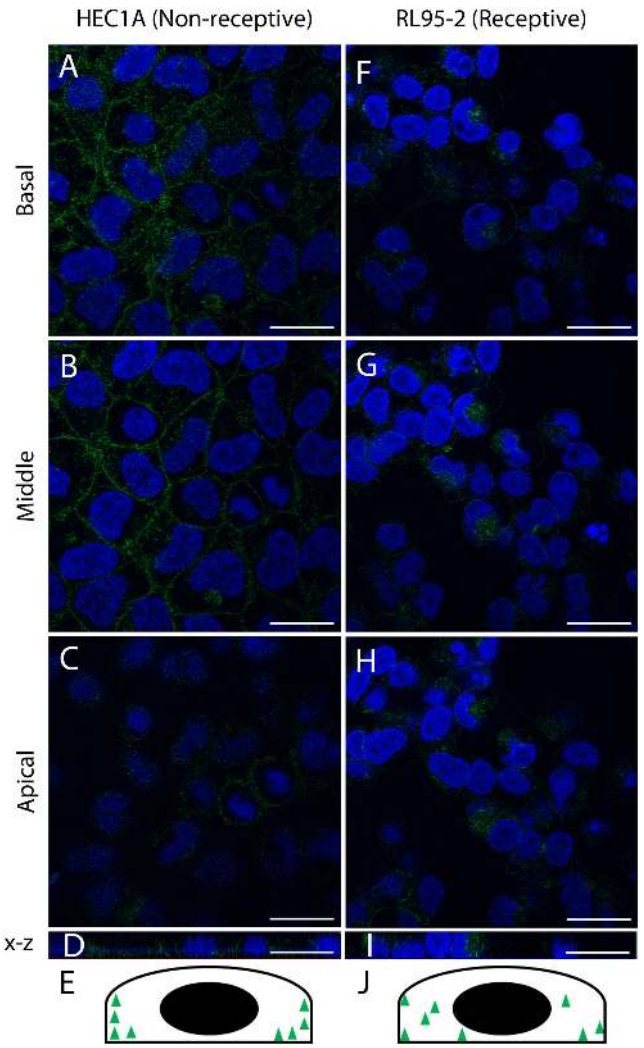

Figure 10 Immunofluorescence confocal microscopy showing Syntaxin 3 localisation in HEC1A and RL95-2 cells treated with cytochalasin D. (A–D) Syntaxin 3 in colchicine treated HEC1A cells was found in all areas of the plasma membrane and the cytoplasm with punctate staining. (F–I) In RL95-2, syntaxin 3 was cytoplasmic is some areas. (D and I) XZ orthogonal plane of Z-stack. (E and J) Schematic diagrams representing VAMP2 localisation in the cells taken from the Z-plane. Scale bars: 20 µm.

the Golgi apparatus are directed to the correct target membrane by t-SNAREs (Mostov *et al.* 2003, Nelson 2003, Rodriguez-Boulan *et al.* 2005). Apically located syntaxin 3 (t-SNARE) traffics vesicular membranes apically and binds to VAMP2 (v-SNARE) to take part in the SNARE complex (Fig. 1). This complex is formed through the coiled coil helix bundles of these proteins allowing the fusion of two opposing membrane bilayers (Bennett *et al.* 1992, Bennett 1995, Nichols *et al.* 1997, Weber *et al.* 1998, Mayer 1999).

This study has shown that syntaxin 3 is localised in the apical cytoplasmic region of UECs on days 3.5, 5.5, 6 and 7. However, the abundance of syntaxin 3 was significantly higher only on day 5.5 compared to day 1 of early pregnancy. The apical localisation of syntaxin 3, as seen in UECs, is consistent with previous studies where syntaxin 3 was also seen apically in human colon epithelial cells and Caco-2 cell lines. In these cells, syntaxin 3 is involved in polarised targeting to the apical plasma membrane (Delgrossi *et al.* 1997, Riento *et al.* 2000). Moreover, syntaxin 3 in UECs during receptivity maintains a high degree of apical polarised localisation, suggesting it may play a role in polarised apical membrane sorting (Riento *et al.* 2000, Sharma *et al.* 2006).

During implantation, there is an increase in sodium ion channel expression in UECs apically to retain maximum fluid absorption (Yang *et al.* 2004,

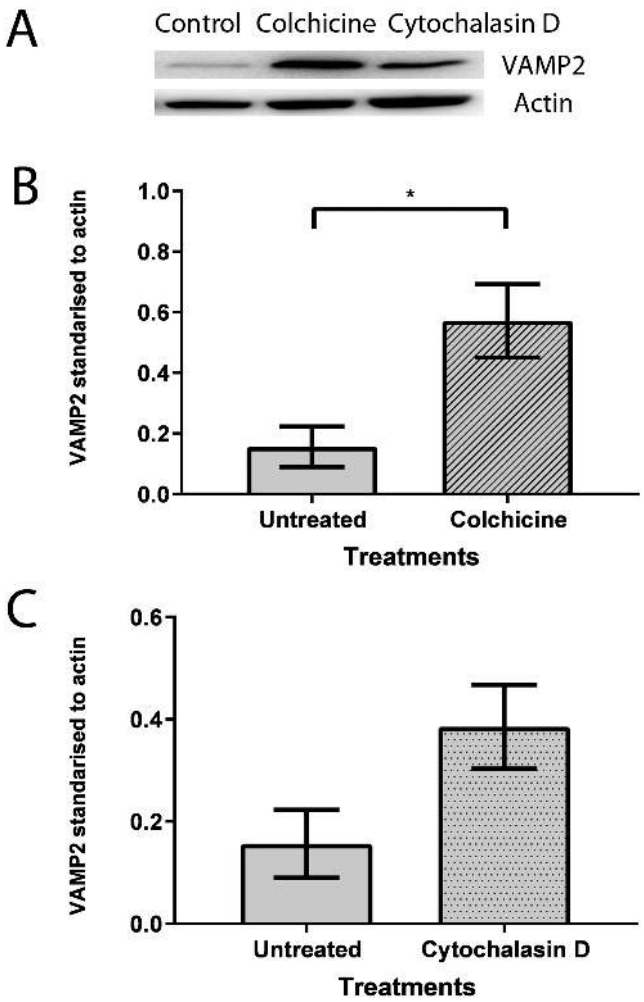

Figure 11 Western blot analysis of VAMP2 in HEC1A cells. (A) VAMP2 was present at 19 kDa when treated with colchicine and cytochalasin D *in vitro*. Actin was used as a loading control. (B) Densitometry and statistical analysis (Student's *t*-test) revealed significantly higher levels of VAMP2 in colchicine-treated HEC1A cell line compared to untreated cells (*$P < 0.05$). (C) The increase in VAMP2 in HEC1A cells was not significant when treated with cytochalasin D compared to untreated cells. Error bar is the mean ± S.E.M., $n = 4$.

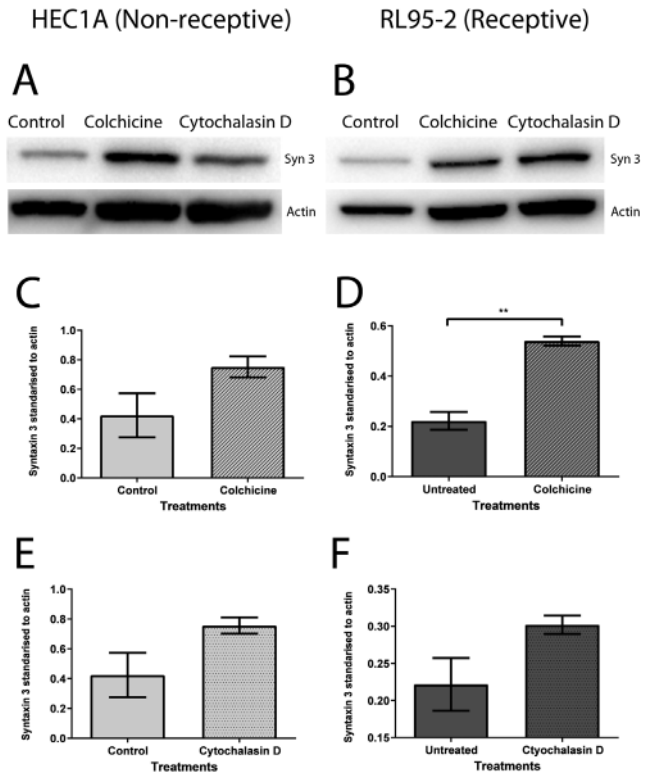

Figure 12 Western blot analysis of syntaxin 3 in human endometrial cell lines. (A and B) Syntaxin 3 was present at 33 kDa when treated with colchicine and cytochalasin D *in vitro*. Actin was used as a loading control. (C) Densitometry analysis and statistical analysis (Student's *t*-test) showed syntaxin 3 had a higher trend in HEC1A colchicine treated cells compared to untreated cells. (D) Syntaxin 3 is significantly higher in colchicine treated RL95-2 cells compared to untreated RL95-2 cells; **$P < 0.01$. (E and F) Syntaxin 3 had an increased trend in HEC1A and RL95-2 cells when actin was disrupted compared to untreated cells. Error bar is the mean ± S.E.M., $n = 4$.

Ruan *et al.* 2014). This aids closure of the total uterine lumen to achieve close apposition between the blastocyst and apical surface of UECs (Lindsay & Murphy 2005, 2006). It is important to note that luminal closure occurs all along the uterine horn and not just in the implantation chamber (Thorpe *et al.* 1974, Png & Murphy 2000). In previous studies, syntaxin 3 has been shown to interact with sodium channels in epithelial cells, where they regulate intrinsic properties and cell-surface expressions of channels (Saxena *et al.* 1999). Thus syntaxin 3 may be involved in both trafficking proteins to the UEC surface required for uterine receptivity and may also assist with the closure of the overall uterine lumen in preparation for apposition via interaction with epithelial sodium channels seen at this time (Chan *et al.* 2002).

Vesicular transport from the Golgi apparatus to any target membrane is dependent on microtubules (Lippincott-Schwartz *et al.* 2000, Sharma *et al.* 2006). Microtubules are reorganised in UECs to facilitate vesicular transport during implantation (Kalam *et al.* 2018). This study examined the effect of microtubule disruption (using colchicine) on VAMP2 and syntaxin 3 in vitro on HEC1A and RL95-2 cells. As expected, colchicine treated cells displayed alterations to both the abundance and localisation of VAMP2 and syntaxin 3. Syntaxin 3 was significantly higher in RL95-2 (receptive) cells compared to HEC1A (non-receptive) cells when treated with colchicine, showing that microtubules influence syntaxin 3 in receptive uterine epithelium. Previous studies that disrupted microtubule tracks found there is an increase in t-SNARE syntaxin 3 signalling. This increase in signalling is thought to compensate for the lack of microtubule tracks and thus achieve the same level of vesicle membrane trafficking that was compromised by colchicine (Kreitzer *et al.* 2003, Schmoranzer & Simon 2003). Therefore, the increase in

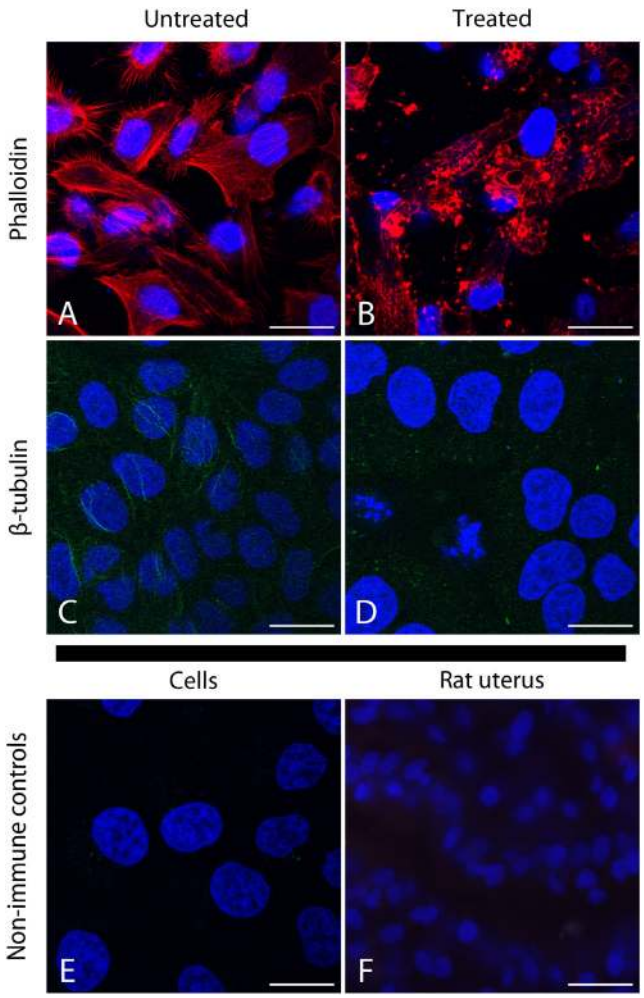

Figure 13 Immunofluorescence of treatment validation and non-immune controls. (A) Intact actin filament bundles (in red shown by Phalloidin labelling) were clearly visible in the non-treated RL95-2 cells. (B) Actin filaments have lost their natural morphology and have become fragmented within the cytoplasm in cytochalasin D treated RL95-2 cells. (C) β-Tubulin stained microtubules (green) can be seen in non-treated HEC1A cells. (D) Colchicine treated HEC1A cells showed absence of microtubule bundles and some β-tubulin punctate staining in the cytoplasm. Non-immune control showed no staining in HEC1A *in vitro* (E) and on day 5.5 *in vivo* (F). Scale bars: 20 μm.

syntaxin 3 observed in this study shows that microtubules may be interacting with the SNARE machinery involved in membrane trafficking and organisation in the receptive RL95-2 cells.

In contrast, actin inhibition had no significant effect on the quantities of VAMP2 or syntaxin 3 in UECs in vitro; however, VAMP2 and syntaxin 3 cellular localisation were affected. Both VAMP2 and syntaxin 3 have a sparse localisation in HEC1A and RL95-2 cells when treated with cytochalasin D, an inhibitor of actin polymerisation. The transition from non-receptive to receptive UECs involves actin distribution to change and maintain its quantity (Luxford & Murphy 1989, 1992). While the actin terminal web structure is lost, actin is still associated with the apical plasma membrane (Moore *et al.* 2016). This actin is referred to as cortical actin and it influences the physiological functions of the plasma membrane (Köster & Mayor 2016). Cortical actin is thought to be involved in the capture and short-range transport of synaptic vesicles at the target plasma membrane (Lang *et al.* 2000, Rudolf *et al.* 2001). At the receptive stage there is a high level of apical vesicular activity shown in this study and this has been observed previously in electron micrograph studies (Parr 1982). Thus, these vesicles are likely to be primarily docking and fusing at the plasma membrane during this stage. During docking time, vesicles are thought to be sensitive to changes in the actin cytoskeleton. Therefore, the change in VAMP2 and syntaxin 3 staining seen particularly in the receptive RL95-2 epithelial cells in the present study could be due to the inhibition of actin polymerisation. In particular, the increase of syntaxin 3 observed with immunofluorescence and Western blotting in RL95-2 (receptive) UECs may be due to the lower actin-membrane association in receptive UECs (Luxford & Murphy 1992, Moore *et al.* 2016). As previous studies have found, actin depolarisation in non-polarised MDCK cells similar to RL95-2 increases calcium-induced lysosomal secretion (Rodríguez *et al.* 1999, Xu *et al.* 2012). Thus, actin organisation in UECs whether as a terminal web, cortical actin or the depolarised may all play a role in SNARE signalling mechanism that controls membrane trafficking.

This study is concerned with changes that occur all along UECs in the transition to uterine receptivity and not those just associated with blastocyst implantation. Technically it would be difficult to image an implantation chamber at day 5.5 of pregnancy in the rat, as the blastocyst sits loosely in a shallow anti-mesometrial depression at this time and is easily dislodged from this position (Enders 1975). Furthermore, it is not until day 6 where the blastocyst adheres to the uterus lining leaving an imprint on the contralateral side, the time in which an implantation chamber can be identified and dissected. This is further supported by the fact that the transient zones do not appear until day 6 of pregnancy in the rat (Krehbiel 1937, Parr *et al.* 1986). Further studies on the role of SNARE proteins directly related to blastocyst and UEC interaction in the future will be needed to establish if there is a role for SNARE proteins in trophoblast-epithelial cell adhesion mechanisms.

In conclusion, the present study has found that the SNARE proteins VAMP2 and syntaxin 3 are involved in membrane trafficking to the apical surface in UECs during early pregnancy. Together VAMP2 and syntaxin 3 may also be involved in the timely trafficking of other membrane proteins such as aquaporin 2, GLUT4 and sodium channels to the apical plasma membrane during the critical stage of UECs where they likely play an important role in uterine receptivity. This study has also

revealed that VAMP2 and syntaxin 3 localisation and abundance are influenced by microtubule organisation as well as cortical actin. These findings advance our understanding of the major membrane trafficking which characterises the apical plasma membrane of UECs during early pregnancy.

Declaration of interest

The authors declare that there is no conflict of interest that could be perceived as prejudicing the impartiality of the research reported.

Funding

Financial support was provided by the Australian Research Council, The Ann Macintosh Foundation of the Discipline of Anatomy and Histology and the Murphy Laboratory.

Author contribution statement

S N K designed the study, performed all experiments, analysed data and took the lead in writing the manuscript. All authors provided critical feedback and helped shape the research, analysis and manuscript.

Acknowledgements

The authors acknowledge the support and facilities of the Bosch Institute Advanced Microscopy Facility, The University of Sydney, and the assistance provided by A/Prof Louise Cole. The authors also acknowledge the support and facilities provided by the Bosch Institute Molecular Biology Facility to Donna Lai and Sheng Hua. The authors also thank members of the Murphy lab.

References

Almers W & Tse FW 1990 Transmitter release from synapses: does a preassembled fusion pore initiate exocytosis? *Neuron* **4** 813–818. (https://doi.org/10.1016/0896-6273(90)90134-2)

Band AM & Kuismanen E 2005 Localization of plasma membrane t-SNAREs syntaxin 2 and 3 in intracellular compartments. *BMC Cell Biology* **6** 26. (https://doi.org/10.1186/1471-2121-6-26)

Baumert M, Maycox PR, Navone F, De Camilli P & Jahn R 1989 Synaptobrevin: an integral membrane protein of 18,000 daltons present in small synaptic vesicles of rat brain. *EMBO Journal* **8** 379–384. (https://doi.org/10.1002/j.1460-2075.1989.tb03388.x)

Bennett MK 1995 SNAREs and the specificity of transport vesicle targeting. *Current Opinion in Cell Biology* **7** 581–586. (https://doi.org/10.1016/0955-0674(95)80016-6)

Bennett MK, Calakos N & Scheller RH 1992 Syntaxin: a synaptic protein implicated in docking of synaptic vesicles at presynaptic active zones. *Science* **257** 255–259. (https://doi.org/10.1126/science.1321498)

Chan LN, Tsang LL, Rowlands DK, Rochelle LG, Boucher RC, Liu CQ & Chan HC 2002 Distribution and regulation of ENaC subunit and CFTR mRNA expression in murine female reproductive tract. *Journal of Membrane Biology* **185** 165–176. (https://doi.org/10.1007/s00232-001-0117-y)

Delgrossi MH, Breuza L, Mirre C, Chavrier P & Le Bivic A 1997 Human syntaxin 3 is localized apically in human intestinal cells. *Journal of Cell Science* **110** 2207–2214.

Dey SK, Lim H, Das SK, Reese J, Paria BC, Daikoku T & Wang H 2004 Molecular cues to implantation. *Endocrine Reviews* **25** 341–373. (https://doi.org/10.1210/er.2003-0020)

Dugani CB, Randhawa VK, Cheng AWP, Patel N & Klip A 2008 Selective regulation of the perinuclear distribution of glucose transporter 4 (GLUT4) by insulin signals in muscle cells. *European Journal of Cell Biology* **87** 337–351. (https://doi.org/10.1016/j.ejcb.2008.02.009)

Duman JG & Forte JG 2003 What is the role of SNARE proteins in membrane fusion? *American Journal of Physiology: Cell Physiology* **285** C237–C249. (https://doi.org/10.1152/ajpcell.00091.2003)

Enders AC 1975 The implantation chamber, blastocyst and blastocyst imprint of the rat: a scanning electron microscope study. *Anatomical Record* **182** 137–149. (https://doi.org/10.1002/ar.1091820202)

Goddette DW & Frieden C 1986 Actin polymerization. The mechanism of action of cytochalasin D. *Journal of Biological Chemistry* **261** 15974–15980.

Hannan NJ, Paiva P, Dimitriadis E & Salamonsen LA 2010 Models for study of human embryo implantation: choice of cell lines? *Biology of Reproduction* **82** 235–245. (https://doi.org/10.1095/biolreprod.109.077800)

Hildenbrand A, Lalitkumar L, Nielsen S, Gemzell-Danielsson K & Stavreus-Evers A 2006 Expression of aquaporin 2 in human endometrium. *Fertility and Sterility* **86** 1452–1458. (https://doi.org/10.1016/j.fertnstert.2006.03.058)

Jahn R & Scheller RH 2006 SNAREs – engines for membrane fusion. *Nature Reviews: Molecular Cell Biology* **7** 631–643. (https://doi.org/10.1038/nrm2002)

Jena BP 2011 Role of SNAREs in membrane fusion. *Advances in Experimental Medicine and Biology* **713** 13–32. (https://doi.org/10.1007/978-94-007-0763-4_3)

Kalam SN, Dowland S, Lindsay L & Murphy CR 2018 Microtubules are reorganised and fragmented for uterine receptivity. *Cell and Tissue Research* **374** 667–677. (https://doi.org/10.1007/s00441-018-2887-x)

Kaneko Y, Lindsay LA & Murphy CR 2008 Focal adhesions disassemble during early pregnancy in rat uterine epithelial cells. *Reproduction, Fertility, and Development* **20** 892–899. (https://doi.org/10.1071/rd08148)

Karvar S, Zhu L, Crothers J, Wong W, Turkoz M & Forte JG 2005 Cellular localization and stimulation-associated distribution dynamics of syntaxin-1 and syntaxin-3 in gastric parietal cells. *Traffic* **6** 654–666. (https://doi.org/10.1111/j.1600-0854.2005.00306.x)

Korgun ET, Demir R, Hammer A, Dohr G, Desoye G, Skofitsch G & Hahn T 2001 Glucose transporter expression in rat embryo and uterus during decidualization, implantation, and early postimplantation. *Biology of Reproduction* **65** 1364–1370. (https://doi.org/10.1095/biolreprod65.5.1364)

Köster DV & Mayor S 2016 Cortical actin and the plasma membrane: inextricably intertwined. *Current Opinion in Cell Biology* **38** 81–89. (https://doi.org/10.1016/j.ceb.2016.02.021)

Krehbiel RH 1937 Cytological studies of the decidual reaction in the rat during early pregnancy and in the production of deciduomata. *Physiological Zoology* **10** 212–234. (https://doi.org/10.1086/physzool.10.2.30160901)

Kreitzer G, Schmoranzer J, Low SH, Li X, Gan Y, Weimbs T, Simon SM & Rodriguez-Boulan E 2003 Three-dimensional analysis of post-Golgi carrier exocytosis in epithelial cells. *Nature Cell Biology* **5** 126–136. (https://doi.org/10.1038/ncb917)

Lang T, Wacker I, Wunderlich I, Rohrbach A, Giese G, Soldati T & Almers W 2000 Role of actin cortex in the subplasmalemmal transport of secretory granules in PC-12 cells. *Biophysical Journal* **78** 2863–2877. (https://doi.org/10.1016/S0006-3495(00)76828-7)

Lindau M & Almers W 1995 Structure and function of fusion pores in exocytosis and ectoplasmic membrane fusion. *Current Opinion in Cell Biology* **7** 509–517. (https://doi.org/10.1016/0955-0674(95)80007-7)

Lindsay LA & Murphy CR 2005 237. Aquaporins in rat uterine epithelial cells during early pregnancy and in response to progesterone. *Reproduction, Fertility and Development* **17** 93. (https://doi.org/10.1071/SRB05Abs237)

Lindsay LA & Murphy CR 2006 Redistribution of aquaporins 1 and 5 in the rat uterus is dependent on progesterone: a study with light and electron microscopy. *Reproduction* **131** 369–378. (https://doi.org/10.1530/rep.1.00914)

Lippincott-Schwartz J, Roberts TH & Hirschberg K 2000 Secretory protein trafficking and organelle dynamics in living cells. *Annual Review of*

Cell and Developmental Biology **16** 557–589. (https://doi.org/10.1146/annurev.cellbio.16.1.557)

Ljungkvist I 1972 Attachment reaction of rat uterine luminal epithelium. IV. The cellular changes in the attachment reaction and its hormonal regulation. *Fertility and Sterility* **23** 847–865. (https://doi.org/10.1016/s0015-0282(16)39318-9)

Low SH, Chapin SJ, Weimbs T, Kömüves LG, Bennett MK & Mostov KE 1996 Differential localization of syntaxin isoforms in polarized Madin-Darby canine kidney cells. *Molecular Biology of the Cell* **7** 2007–2018. (https://doi.org/10.1091/mbc.7.12.2007)

Low SH, Chapin SJ, Wimmer C, Whiteheart SW, Kömüves LG, Mostov KE & Weimbs T 1998 The SNARE machinery is involved in apical plasma membrane trafficking in MDCK cells. *Journal of Cell Biology* **141** 1503–1513. (https://doi.org/10.1083/jcb.141.7.1503)

Low SH, Vasanji A, Nanduri J, He M, Sharma N, Koo M, Drazba J & Weimbs T 2006 Syntaxins 3 and 4 are concentrated in separate clusters on the plasma membrane before the establishment of cell polarity. *Molecular Biology of the Cell* **17** 977–989. (https://doi.org/10.1091/mbc.e05-05-0462)

Luxford KA & Murphy CR 1989 Cytoskeletal alterations in the microvilli of uterine epithelial cells during early pregnancy. *Acta Histochemica* **87** 131–136. (https://doi.org/10.1016/S0065-1281(89)80015-7)

Luxford KA & Murphy CR 1992 Reorganization of the apical cytoskeleton of uterine epithelial cells during early pregnancy in the rat: a study with myosin subfragment 1. *Biology of the Cell* **74** 195–202. (https://doi.org/10.1016/0248-4900(92)90025-v)

Martín JC, Jasper MJ, Valbuena D, Meseguer M, Remohí J, Pellicer A & Simón C 2000 Increased adhesiveness in cultured endometrial-derived cells is related to the absence of moesin expression. *Biology of Reproduction* **63** 1370–1376. (https://doi.org/10.1095/biolreprod63.5.1370)

Martinez-Arca S, Lalioti VS & Sandoval IV 2000 Intracellular targeting and retention of the glucose transporter GLUT4 by the perinuclear storage compartment involves distinct carboxyl-tail motifs. *Journal of Cell Science* **113** 1705–1715.

Mayer A 1999 Intracellular membrane fusion: SNAREs only? *Current Opinion in Cell Biology* **11** 447–452. (https://doi.org/10.1016/S0955-0674(99)80064-7)

Mendez M, Gross KW, Glenn ST, Garvin JL & Carretero OA 2011 Vesicle-associated membrane protein-2 (VAMP2) mediates cAMP-stimulated renin release in mouse juxtaglomerular cells. *Journal of Biological Chemistry* **286** 28608–28618. (https://doi.org/10.1074/jbc.M111.225839)

Moore CL, Cheng D, Shami GJ & Murphy CR 2016 Correlated light and electron microscopy observations of the uterine epithelial cell actin cytoskeleton using fluorescently labeled resin-embedded sections. *Micron* **84** 61–66. (https://doi.org/10.1016/j.micron.2016.02.010)

Mostov K, Su T & ter Beest M 2003 Polarized epithelial membrane traffic: conservation and plasticity. *Nature Cell Biology* **5** 287–293. (https://doi.org/10.1038/ncb0403-287)

Murphy CR 1993 The plasma membrane of uterine epithelial cells: structure and histochemistry. *Progress in Histochemistry and Cytochemistry* **27** 1–66. (https://doi.org/10.1016/s0079-6336(11)80004-5)

Murphy CR 2004 Uterine receptivity and the plasma membrane transformation. *Cell Research* **14** 259–267. (https://doi.org/10.1038/sj.cr.7290227)

Murphy CR & Shaw TJ 1994 Plasma membrane transformation: a common response of uterine epithelial cells during the peri-implantation period. *Cell Biology International* **18** 1115–1128. (https://doi.org/10.1006/cbir.1994.1038)

Nelson WJ 2003 Adaptation of core mechanisms to generate cell polarity. *Nature* **422** 766–774. (https://doi.org/10.1038/nature01602)

Nichols BJ, Ungermann C, Pelham HRB, Wickner WT & Haas A 1997 Homotypic vacuolar fusion mediated by t- and v-SNAREs. *Nature* **387** 199–202. (https://doi.org/10.1038/387199a0)

Nielsen S, Marples D, Birn H, Mohtashami M, Dalby NO, Trimble M & Knepper M 1995 Expression of VAMP-2-like protein in kidney collecting duct intracellular vesicles. Colocalization with aquaporin-2 water channels. *Journal of Clinical Investigation* **96** 1834–1844. (https://doi.org/10.1172/JCI118229)

Nilsson BO & Lundkvist O 1979 Ultrastructural and histochemical changes of the mouse uterine epithelium on blastocyst activation for implantation. *Anatomy and Embryology* **155** 311–321. (https://doi.org/10.1007/BF00317644)

Pantaleon M & Kaye PL 1998 Glucose transporters in preimplantation development. *Reviews of Reproduction* **3** 77–81. (https://doi.org/10.1530/ror.0.0030077)

Parr MM 1982 Apical vesicles in the rat uterine epithelium during early pregnancy: a morphometric study. *Biology of Reproduction* **26** 915–924. (https://doi.org/10.1095/biolreprod26.5.915)

Parr MB, Tung HN & Parr EL 1986 The ultrastructure of the rat primary decidual zone. *American Journal of Anatomy* **176** 423–436. (https://doi.org/10.1002/aja.1001760405)

Peng XR, Yao X, Chow DC, Forte JG & Bennett MK 1997 Association of syntaxin 3 and vesicle-associated membrane protein (VAMP) with H+/K(+)-ATPase-containing tubulovesicles in gastric parietal cells. *Molecular Biology of the Cell* **8** 399–407. (https://doi.org/10.1091/mbc.8.3.399)

Png FY & Murphy CR 2000 Closure of the uterine lumen and the plasma membrane transformation do not require blastocyst implantation. *European Journal of Morphology* **38** 122–127. (https://doi.org/10.1076/0924-3860(200004)38:2;1-f;ft122)

Ramm G, Slot JW, James DE & Stoorvogel W 2000 Insulin recruits GLUT4 from specialized VAMP2-carrying vesicles as well as from the dynamic endosomal/trans-Golgi network in rat adipocytes. *Molecular Biology of the Cell* **11** 4079–4091. (https://doi.org/10.1091/mbc.11.12.4079)

Randhawa VK, Bilan PJ, Khayat ZA, Daneman N, Liu Z, Ramlal T, Volchuk A, Peng XR, Coppola T, Regazzi R *et al.* 2000 VAMP2, but not VAMP3/cellubrevin, mediates insulin-dependent incorporation of GLUT4 into the plasma membrane of L6 myoblasts. *Molecular Biology of the Cell* **11** 2403–2417. (https://doi.org/10.1091/mbc.11.7.2403)

Riento K, Kauppi M, Keränen S & Olkkonen VM 2000 Munc18-2, a functional partner of syntaxin 3, controls apical membrane trafficking in epithelial cells. *Journal of Biological Chemistry* **275** 13476–13483. (https://doi.org/10.1074/jbc.275.18.13476)

Rodríguez A, Martinez I, Chung A, Berlot CH & Andrews NW 1999 cAMP regulates Ca2+-dependent exocytosis of lysosomes and lysosome-mediated cell invasion by trypanosomes. *Journal of Biological Chemistry* **274** 16754–16759. (https://doi.org/10.1074/jbc.274.24.16754)

Rodriguez-Boulan E, Kreitzer G & Müsch A 2005 Organization of vesicular trafficking in epithelia. *Nature Reviews: Molecular Cell Biology* **6** 233–247. (https://doi.org/10.1038/nrm1593)

Rossetto O, Gorza L, Schiavo G, Schiavo N, Scheller RH & Montecucco C 1996 Vamp/synaptobrevin isoforms 1 and 2 are widely and differentially expressed in nonneuronal tissues. *Journal of Cell Biology* **132** 167–179. (https://doi.org/10.1083/jcb.132.1.167)

Ruan YC, Chen H & Chan HC 2014 Ion channels in the endometrium: regulation of endometrial receptivity and embryo implantation. *Human Reproduction Update* **20** 517–529. (https://doi.org/10.1093/humupd/dmu006)

Rudolf R, Salm T, Rustom A & Gerdes HH 2001 Dynamics of immature secretory granules: role of cytoskeletal elements during transport, cortical restriction, and F-actin-dependent tethering. *Molecular Biology of the Cell* **12** 1353–1365. (https://doi.org/10.1091/mbc.12.5.1353)

Saxena S, Quick MW, Tousson A, Oh Y & Warnock DG 1999 Interaction of syntaxins with the amiloride-sensitive epithelial sodium channel. *Journal of Biological Chemistry* **274** 20812–20817. (https://doi.org/10.1074/jbc.274.30.20812)

Schlafke S & Enders AC 1975 Cellular basis of interaction between trophoblast and uterus at implantation. *Biology of Reproduction* **12** 41–65. (https://doi.org/10.1095/biolreprod12.1.41)

Schlafke S, Welsh AO & Enders AC 1985 Penetration of the basal lamina of the uterine luminal epithelium during implantation in the rat. *Anatomical Record* **212** 47–56. (https://doi.org/10.1002/ar.1092120107)

Schmoranzer J & Simon SM 2003 Role of microtubules in fusion of post-Golgi vesicles to the plasma membrane. *Molecular Biology of the Cell* **14** 1558–1569. (https://doi.org/10.1091/mbc.e02-08-0500)

Schoch S, Deák F, Königstorfer A, Mozhayeva M, Sara Y, Südhof TC & Kavalali ET 2001 SNARE function analyzed in synaptobrevin/VAMP

knockout mice. *Science* **294** 1117–1122. (https://doi.org/10.1126/science.1064335)

Scott AI 1960 Biosynthesis of colchicine. *Nature* **186** 556. (https://doi.org/10.1038/186556a0)

Sharma N, Low SH, Misra S, Pallavi B & Weimbs T 2006 Apical targeting of syntaxin 3 is essential for epithelial cell polarity. *Journal of Cell Biology* **173** 937–948. (https://doi.org/10.1083/jcb.200603132)

Söllner T, Whiteheart SW, Brunner M, Erdjument-Bromage H, Geromanos S, Tempst P & Rothman JE 1993 SNAP receptors implicated in vesicle targeting and fusion. *Nature* **362** 318–324. (https://doi.org/10.1038/362318a0)

Soo Hoo L, Banna CD, Radeke CM, Sharma N, Albertolle ME, Low SH, Weimbs T & Vandenberg CA 2016 The SNARE protein syntaxin 3 confers specificity for polarized axonal trafficking in neurons. *PLoS ONE* **11** e0163671. (https://doi.org/10.1371/journal.pone.0163671)

Sutton RB, Fasshauer D, Jahn R & Brunger AT 1998 Crystal structure of a SNARE complex involved in synaptic exocytosis at 2.4 A resolution. *Nature* **395** 347–353. (https://doi.org/10.1038/26412)

Tajika Y, Sato M, Murakami T, Takata K & Yorifuji H 2007 VAMP2 is expressed in muscle satellite cells and up-regulated during muscle regeneration. *Cell and Tissue Research* **328** 573–581. (https://doi.org/10.1007/s00441-006-0376-0)

Takata K, Matsuzaki T & Tajika Y 2004 Aquaporins: water channel proteins of the cell membrane. *Progress in Histochemistry and Cytochemistry* **39** 1–83. (https://doi.org/10.1016/j.proghi.2004.03.001)

ter Beest MB, Chapin SJ, Avrahami D & Mostov KE 2005 The role of syntaxins in the specificity of vesicle targeting in polarized epithelial cells. *Molecular Biology of the Cell* **16** 5784–5792. (https://doi.org/10.1091/mbc.e05-07-0661)

Thorpe LW, Connors TJ & Soderwall AL 1974 Closure of the uterine lumen at implantation in senescent golden hamsters. *Journal of Reproduction and Fertility* **39** 29–32. (https://doi.org/10.1530/jrf.0.0390029)

Ungermann C & Langosch D 2005 Functions of SNAREs in intracellular membrane fusion and lipid bilayer mixing. *Journal of Cell Science* **118** 3819–3828. (https://doi.org/10.1242/jcs.02561)

Watson RT & Pessin JE 2001 Transmembrane domain length determines intracellular membrane compartment localization of syntaxins 3, 4, and 5. *American Journal of Physiology: Cell Physiology* **281** C215–C223. (https://doi.org/10.1152/ajpcell.2001.281.1.C215)

Watson RT, Kanzaki M & Pessin JE 2004 Regulated membrane trafficking of the insulin-responsive glucose transporter 4 in adipocytes. *Endocrine Reviews* **25** 177–204. (https://doi.org/10.1210/er.2003-0011)

Weber T, Zemelman BV, McNew JA, Westermann B, Gmachl M, Parlati F, Söllner TH & Rothman JE 1998 SNAREpins: minimal machinery for membrane fusion. *Cell* **92** 759–772. (https://doi.org/10.1016/s0092-8674(00)81404-x)

Xu J, Toops KA, Diaz F, Carvajal-Gonzalez JM, Gravotta D, Mazzoni F, Schreiner R, Rodriguez-Boulan E & Lakkaraju A 2012 Mechanism of polarized lysosome exocytosis in epithelial cells. *Journal of Cell Science* **125** 5937–5943. (https://doi.org/10.1242/jcs.109421)

Yang JZ, Ajonuma LC, Tsang LL, Lam SY, Rowlands DK, Ho LS, Zhou CX, Chung YW & Chan HC 2004 Differential expression and localization of CFTR and ENaC in mouse endometrium during pre-implantation. *Cell Biology International* **28** 433–439. (https://doi.org/10.1016/j.cellbi.2004.03.011)

Received 27 April 2020
First decision 13 May 2020
Revised manuscript received 7 July 2020
Accepted 17 July 2020